DEVELOPMENT OF DISK-AND-WASHER CAVITY IN KEK

S. Inagaki, T. Higo, K. Takata, H. Nakanishi, S. Noguchi, T. Furuya
K. Kitagawa, E. Ezura, Y. Kojima and T. Takashima
National Laboratory for High Energy Physics
Oho-machi, Tsukuba-gun, Ibaraki-ken, 305, Japan

Summary

The behavior of the deflecting mode of the disk and washer structure was studied experimentally and computationally. A possibility was proved that the second HEM_1 passband can be moved above the accelerating frequency and that the value of R/Q can be increased by 60 % compared to that of the shunt impedance optimized DAW cavity, if one makes a compromise with 80 % of the optimized shunt impedance. The transverse coupling impedance of the second HEM_1 mode at π phase shift is less than 1 Mohm/m for a single cell, which is small by more than an order of magnitude compared to that of the re-entrant cavity or disk loaded cavity.

Introduction

Notwithstanding the extensive studies throughout the world since the proposal of the disk and washer (DAW) structure,[1] the actual application to the practical accelerator has not yet been realized.

The first difficulty was encountered in the supporting stem of the washer, which degraded the quality value or violated the symmetry of the field distribution. In other words the problem of the stem could not be treated as a perturbation. However, we found that with a single radial stem at least 80 % of the calculated shunt impedance can be obtained overall.[2]

The overlapping of passbands at the accelerating frequency is another problem.[2,3,4] Especially the second HEM_1 passband may cause serious problems for a cavity with many coupled cells. To study the general bahavior of the deflecting mode, the dispersion characteristics were measured for six types of cavities.

The displacement of the beam from the axis excites deflecting modes and they may cause the beam blow-up problem. Therefore, as a figure of merit, the transverse coupling impedance was measured.

When these measurements had almost been completed the computer code URMEL[5] was kindly supplied by Weiland. It can solve the non-axially symmetric electromagnetic field in an axially symmetric cavity. The calculated results are referred in analysing the measurements and obtaining the transverse coupling impedance.

Description of the Model Cavities

The geometrical sizes of six types of cavities are shown in Table I with their notations in Fig. 1. They were designed by the aid of SUPERFISH[6] to be confluent for both the accelerating and coupling mode at 500 MHz. The bore hole diameter is required not to be less than 10.0 cm by the lattice design. Eventhough the model cavities were scaled down to 1/3, the measured values reported here are converted into those of the actual size. Twelve cells including full end cells[7] were prepared for Type A. Six cells terminated at the middle of the disk and at the middle of the washer were prepared for Type B. Two cells with the same termination as above were prepared for others.

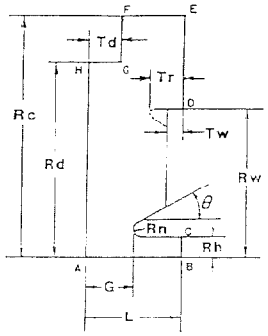

Fig. 1
Notations of DAW cavity

Type A cavity is the optimized one in the shunt impedance. The basic studies in Ref. 2 were done for this type.

Type B is designed[8] as the extreme case of the DAW structure in the sense that the inner radius of the disk is reduced to the outer radius of the washer, and the second HEM_1 passband is expected to lie far above the accelerating frequency. Because of the narrow slot between the accelerating and coupling cavity, the band width of HEM_1 mode is intended to be smaller than that of Type A. Furthermore the disturbance to the accelerating mode due to the stem can be expected to be small, because the electric field from the washer concentrates to the disk rather than to the outer cylinder. Type E uses the same washer as Type B. The taper of the disk is strongly demanded by the technical point of view, i.e. the electroplating and welding of the stem to the outer cylinder. Type D has no rim at the washer and has nearly the same size as Type B.

Type C cavity is designed to have an intermediate shunt impedance between A and B with the second HEM_1 passband above the accelerating freqeuncy.

Type X cavity has no disk and operates in π mode (Fig. 2). The grooves at the outer surface of the washer is needed to make confluent.[9]

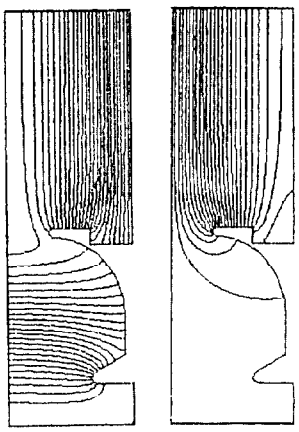

Fig. 2 Accelerating (left) and coupling (right) mode of Type X cavity

Table I Six types of DAW cavity

Type	A	B	C	D	E	X
Rc(cm)	45.45	33.36	40.0	34.09	35.35	50.0
Rd(cm)	40.25	25.0	33.0	25.0	25.0	
Td(cm)	7.2	10.0	9.25	9.26	11.7	
G (cm)	10.25	10.51	10.85	8.97	10.51	10.0
Rw(cm)	24.45	25.0	25.0	25.0	25.0	23.46
Tw(cm)	0.95	1.0	1.0	1.0	1.0	1.0
Tr(cm)	0.95	2.5	1.0	1.0	2.5	10.0
Rh(cm)	5.0	5.0	5.0	5.0	5.0	5.0
L (cm)	15.0	15.0	15.0	15.0	15.0	15.0
T	0.765	0.759	0.754	0.793	0.760	0.769
R(Mohm/m)	76.49	60.07	72.55	56.96	60.28	55.41
RT^2(Mohm/m)	44.76	34.59	41.19	35.81	34.79	32.77
P(kw)	3.922	4.996	4.036	5.266	4.977	5.415
Q(x10^4)	11.25	5.447	9.096	5.597	5.442	7.507
R/Q(kohm/m)	0.680	1.10	0.797	1.02	1.11	0.738

Dispersion Properties

The details of the mode assignment process are described in Ref. 7.

In Fig. 3-8 are shown the dispersion curves of all types of cavities and those of washer removed cavities for Type A, B and C. The calculated modes of the cylindrical cavities with the average radius are also shown for Type A, B and C.

In the case of Type B, the unfavourable modes are cleared out around the accelerating frequency, while in Type A, four passbands cross the accelerating frequency. Practically, Type C cavity is found to be the worst one with regard to the mode overlapping. Compared to Type

0018-9499/83/0800-3572$01.00© 1983 IEEE

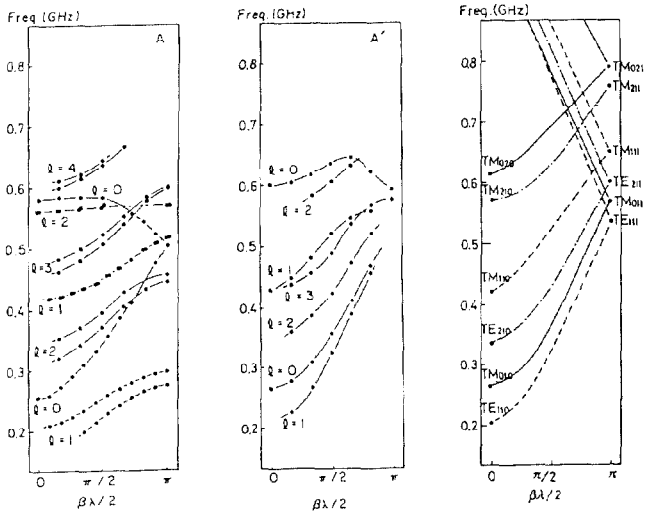

Fig. 3 Dispersion curves of Type A, washer-removed Type A and cylindrical cavity (L-R).

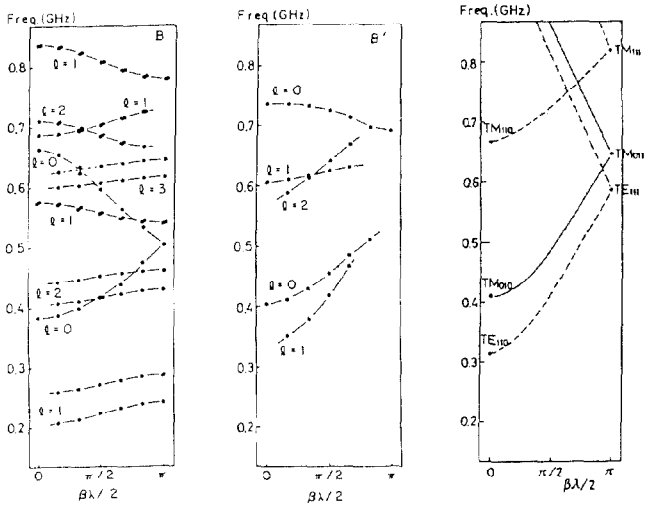

Fig. 4 Dispersion curves of Type B, washer-removed Type B and cylindrical cavity (L-R).

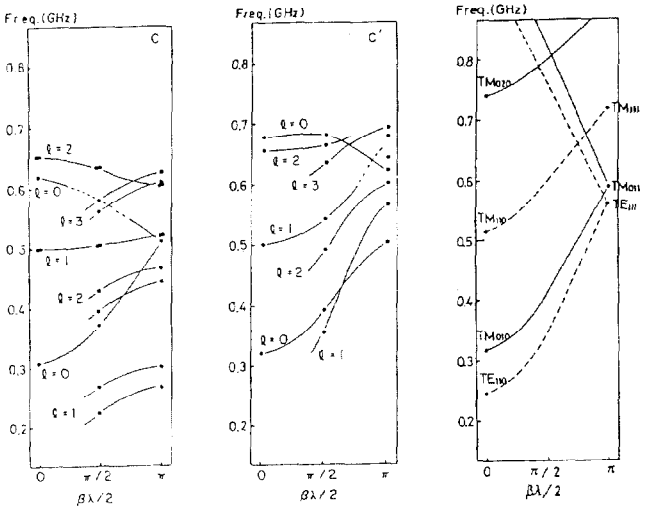

Fig. 5 Dispersion curves of Type C, washer-removed Type C and cylindrical cavity (L-R).

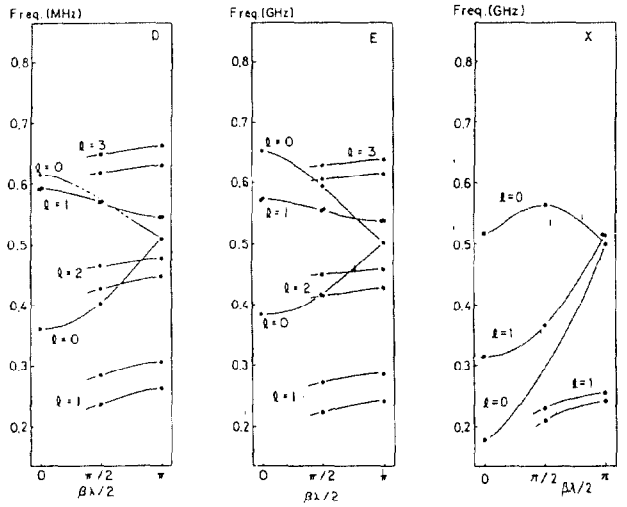

Fig. 6 Fig. 7 Fig. 8

Dispersion curves of Type D, E and X (L-R)

B, Type D cavity has higher frequency for HEM_1 and HEM_2 mode and lower frequency for TM_{010} and TM_{020}. Type E behaves almost the same as Type B. From Figs. 3 to 5, the passbands of DAW could be understood from those of pillbox cavity as follows. The lower passband of DAW TM_0 comes from pillbox TM_{010}-TM_{011}, while the upper passband of DAW TM_0 comes from the mixture of pillbox TM_{020}-TM_{011}. The first DAW HEM_1 originates from pillbox TE_{110}-TE_{111}. The second DAW HEM_1 originates from the mixture of pillbox TM_{110}-TE_{111}. This fact is also shown in the field distribution calculated by URMEL for Type A cavity (Fig. 9). For 0-mode, the field distribution near the axis resembles that of TM mode and for π-mode, it resembles that of TE mode. In the case of Type B, the situation is not so much different. For 0-mode it looks like TM and for π-mode, it still looks like TE in spite of the strong effect of the washer rim (Fig. 10).

Transverse Coupling Impedance

For Type A cavity, the second HEM_1 passband crosses the accelerating frequency near π-mode, and even for Type B cavity it intersects v = c line around this region. As a figure of merit of deflecting mode, the transverse shunt impedance R_t was measured. It is derived from the transverse coupling impedance

$$Z_t(\omega) = \lim_{\Delta \to 0} \left(\int [E + v \times B]_t \exp(jkz) dz / I\Delta \right) ,$$

where $k = \omega/c$, I is the beam current and Δ, the displacement form the equilibrium orbit. After some manipulation,[10] it follows that

$$Z_t = \frac{R_t \omega_a/\omega}{1 + jQ_a(\omega/\omega_a - \omega_a/\omega)} ,$$

where

$$R_t = Q_a c |v_t|^2 / \varepsilon \omega_a^2 ,$$

and

$$v_t = - \int (\text{grad } E_{az})_t \cdot \exp(jkz) dz .$$

In Table II, the comparison is made between measured and calculated R_t/Q of the second HEM_1-0 mode for three types of cavities, and they agree within ± 8 %.

In Table III, the measured freqeuncy, the calculated frequency, Q-value, R_t/Q and R_t are listed for HEM_1 mode.

Discussion

The frequency of the second HEM_1-0 mode can be scaled by the average radius of the cavity for the shape like Type A or C within a few percent. For Type B, D and E, the frequency is lower than that expected from the scaling by about 12 %. In all model cavities, the second HEM_1-π mode lies above the accelerating mode and the frequency difference is almost constant. It is about + 2.5 % for Type A and C, and about + 7 % for Type B, D and E. We do not have any rule to explain this behavior yet.

The transverse shunt impedance of the second HEM_1-π mode are calculated for DAW, re-entrant and disk loaded cavity and shown in Table IV. In the case of DAW structure, it is smaller by more than an order of magnitude than those of other cavities.[11] This is qualitatively explained by the field distribution near the axis. That of DAW is TE-like, while those of the others are TM like.

Two 12-cell Type A cavities to be installed in the TRISTAN accumulator ring are under construction. According to the model cavity measurement, the resonances exist at 508.1 MHz (HEM_1) and 502.9 MHz (HEM_3) near the accelerating freqeuncy (504.5 MHz), and the elaborate study is in progress for the actual cavity.

In Type B cavity, 1) the unfavourable passbands are more than 33 MHz apart from the accelerating frequency, 2) the coupling constant of the second HEM_1 mode is small (k = 0.06), 3) the R/Q of the accelerating mode is high (1.1 kohm/m) compared to that of Type A (0.6 kohm/m) and 4) the transverse coupling impedance of the second HEM_1-π mode is still small ($\leq$ 1 Mohm/m). The structure similar to Type B is recommended if one can make a compromise with about 80 % of the optimized shunt impedance.

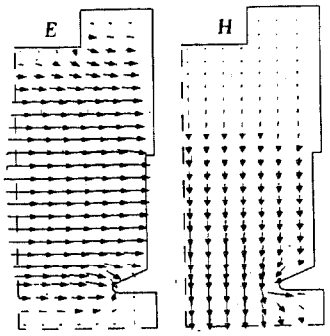

Fig. 9(a)
Second HEM_1-0 mode of Type A.

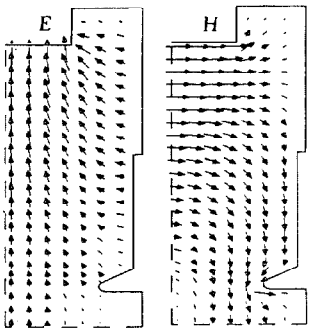

Fig. 9(b)
Second HEM_1-π mode of Type A.

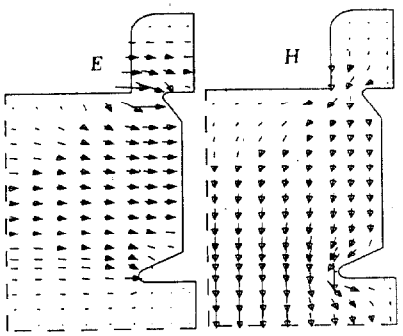

Fig.10(a)
Second HEM_1-0 mode of Type B.

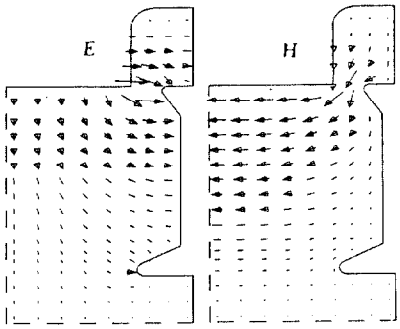

Fig.10(b)
Second HEM_1-π mode of Type B.

Table *II* Measured and calculated R_t/Q.

Type	R_t/Q(ohm/m) meas.	calc.
A	309	312
B	218	237
C	364	343

Table *IV* Transeverse coupling impedance of HEM_1-π mode of typical cavity structure

Cavity Type	Freq.(MHz)	R_t(Mohm/m)
DAW-A	514	0.35
DAW-B	533	0.63
re-entrant	1069	33.
disk loaded	741	20.

Table *III* Frequency, Q, R_t/Q and R_t of HEM_1-mode of DAW cavity.

Cavity Type	Mode	Frequency meas. (MHz)	Frequency calc. (MHz)	Q ($\times 10^4$)	R_t/Q (ohm/m)	R_t (Mohm/m)
A	1st HEM1-0	153	160	4.47	4.52	0.20
A	1st HEM1-π	241	275	5.92	436.	26.
A	2nd HEM1-0	422	424	6.34	313.	20.
A	2nd HEM1-π	517	514	5.45	6.45	0.35
A	3rd HEM1-0		620	4.65	2.98	0.14
A	3rd HEM1-π		648	5.38	0.90	0.05
A	4th HEM1-0		750	6.58	194.	13.
A	4th HEM1-π		640	11.5	171.	20.
B	1st HEM1-0	203	204	1.32	9.36	0.12
B	1st HEM1-π	241	239	1.78	296.	5.3
B	2nd HEM1-0	576	567	2.47	237.	5.9
B	2nd HEM1-π	539	533	2.10	30.	0.63
B	3rd HEM1-0	686	682	5.02	0.25	0.05
B	3rd HEM1-π	693	722	4.28	4.44	0.19
B	4th HEM1-0	835	826	5.14	208.	11.
B	4th HEM1-π	779	776	6.36	346.	22.
C	2nd HEM1-0	498	500	4.79	343.	16.
C	2nd HEM1-π	523	519	4.60	6.12	0.28

Acknowledgement

We express our sincere thanks to Dr. Weiland at DESY for providing URMEL. We also appreciate Drs. R. Jameson, D. Swenson and Y. Iwashita of LANL for sending the informations of their work.

References

1. Y.G. Andreev, I.G. Guslitskov, E.A. Mirochnik, V.M. Pirozhenko and B.I. Polyakov, Proc. 1976 Linac Conf. AECL-5677 (1976).
2. K. Takata, S. Inagaki, H. Nakanishi, K. Kitagawa, H. Ishimaru, Y. Yamazaki and P. Grand, IEEE Trans. Nucl. Sci. NS-28, 2873 (1981).
3. L. Young and J. Potter, LANL memorandum, AT-1: 59 (1982).
4. Y. Iwashita, LANL Memorandum, AT-DO: YI-234.
5. T. Weiland, DESY M-82-24, Oct. (1982).
6. K. Halbach and R.F. Holsinger, Particle Accelerator 7, 213 (1976).
7. T. Higo, S. Inagaki, K. Takata, H. Nakanishi, K. Kitagawa, S. Noguchi and T. Furuya, Proc. 7th Meeting on Linear Accelerators, KEK-82-14, p.135 (1983) (in Japanese).
8. S. Inagaki, T. Higo, K. Takata and H. Nakanishi, Proc. 4th Symposium on Accelerator Science and Technology, IPCR (Wako-shi), p.257 (1982).
9. S. Inagaki, KEK-81-4 (1981).
10. T. Suzuki: private communication.
11. For the experimental data of a re-entrant cavity, see Y. Yamazaki, K. Takata and S. Tokumoto, KEK 80-8 (1980).